Direct Measurement of Strain-Induced Changes in the Band Structure of Carbon Nanotubes

Mingyuan Huang,[1] Yang Wu,[2] Bhupesh Chandra,[1] Hugen Yan,[2] Yuyao Shan,[1] Tony F. Heinz,[2] and James Hone[1]

[1]*Department of Mechanical Engineering, Columbia University, New York, New York, 10027 USA*

[2]*Department of Physics and Electrical Engineering, Columbia University, New York, New York, 10027 USA*

(Received 26 October 2007; published 3 April 2008)

The effect of uniaxial strain on the optical transition energies of single-walled carbon nanotubes with known chiral indices was measured by Rayleigh scattering spectroscopy. Existing theory accurately predicts the trends in the measured strain-induced shifts, but overestimates their magnitude. Modification of the analysis to account for internal sublattice relaxation results in quantitative agreement with experiment.

DOI: 10.1103/PhysRevLett.100.136803 PACS numbers: 73.63.Fg, 78.67.Ch, 81.05.Tp

The electronic properties of carbon nanotubes are uniquely sensitive to geometry, with either semiconducting or metallic band structure possible, depending on the exact (n, m) chiral indices [1]. A consequence of this sensitivity is the existence of strong and unusual electromechanical effects whose magnitude and sign are predicted to depend on the chiral indices [2–6]. Previous experimental studies [7–11] have provided qualitative confirmation of theoretical predictions, but quantitative comparison has been difficult because of a lack of independent knowledge of the nanotube crystal structure. Accurate determination of these effects is important for nanotube electromechanical devices, as well as understanding of electron-phonon scattering and environmental perturbations.

In this Letter, we present measurements of strain-induced changes in the electronic structure of individual single-walled carbon nanotubes (SWNTs). The shifts are qualitatively consistent with existing theory. At the *quantitative* level, however, previous theoretical treatments significantly overestimate the strain-induced energy shifts. Through a modification of the earlier treatment to account for sublattice relaxation using existing atomic interaction potentials, we obtain excellent agreement with experiment without the introduction of any adjustable parameter.

Rayleigh scattering spectroscopy [12], which measures the frequency-dependent scattering of white light from a single freely suspended nanotube, was used for the precise measurement of the effect of strain on the optical transition energies, as well as for identification of the nanotube crystal structure. For the nanotubes studied in this work (with diameters of 2.1–2.4 nm) and the available spectral range, we observed scattering peaks corresponding to the third and fourth optical transitions (S_{33} and S_{44}) for semiconducting nanotubes and the second optical transition (M_{22}) for metallic ones. The positions of these peaks permit the determination of unique (n, m) indices for the spectra. The assignments are based on previous studies that employed independent structural determination by electron diffraction [13] and are also consistent with Kataura plot patterns found by photoluminescence and resonant Raman spectroscopy [14,15].

Because Rayleigh spectroscopy requires suspended samples to eliminate background optical signal, previous studies have used SWNTs grown over slits etched through Si wafers [12] with a thin Si_3N_4 epilayer. In this work, the single slit was replaced by an "H" shape [Fig. 1(a)]. Chemical vapor deposition was used to grow long (~mm total length) nanotubes that aligned with the CVD gas flow and spanned the ~100 μm wide central slit. The sample growth procedure and geometry have been described in

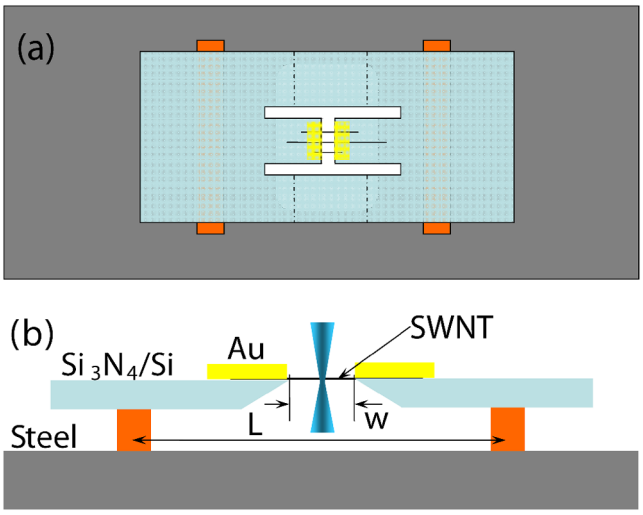

FIG. 1 (color online). Schematic representation of the device structure (not to scale). (a, top view) SWNTs are grown across the middle of an H-shaped slit in a Si wafer, and clamped at the ends by gold films. The Si chip is glued to a piece of steel with two attachment pads. The Si chip is then cut along the dashed lines to separate the two halves of the wafer. (b, side view) Light for Rayleigh scattering is focused on a suspended SWNT from the top; the scattered light is collected after passing through the slit and a hole in steel plate (not visible). Typical values for the slit width w and the chip length L were 100 μm and 12 mm, respectively.

detail previously [16]. When a suitable nanotube (i.e., clean, straight, and not bundled with other nanotubes) was identified by Rayleigh spectroscopy, gold was evaporated through a shadow mask to clamp it to the substrate. The chip was then glued at its ends to a thin steel plate, with a hole underneath the central slit. Finally, the chip was carefully cut using a diamond scribe [along the dashed lines in Fig. 1(a)], leaving the nanotube suspended between two separate pieces of the Si wafer [Fig. 1(b)].

Axial strain was applied to the nanotube by heating the steel base plate. Differential thermal expansion places the nanotube under axial strain $\varepsilon = (\alpha_{\text{steel}} - \alpha_{\text{Si}})\Delta T(L/w)$, where ΔT is the temperature increase, $\alpha_{\text{steel}} \sim 13 \times 10^{-6}\ \text{K}^{-1}$ and $\alpha_{\text{Si}} \sim 2.6 \times 10^{-6}\ \text{K}^{-1}$ are the room-temperature thermal expansion coefficients, and $(L/w) \sim 12\ \text{mm}/100\ \mu\text{m}$ is the ratio of the separation between two steel-Si attachment points to the width of slit. For typical devices, this yields a rate change of nanotube strain with temperature of $0.12\%\ \text{K}^{-1}$. This rate was confirmed by direct measurement of the slit width upon heating. Because the nanotube's thermal expansion coefficient is of order $10^{-5}\ \text{K}^{-1}$ [17], we can neglect this effect in our analysis. In a separate study [18], we have determined that the built-in strain (or slack) in the as-grown nanotubes is less than 0.01%, which is not high enough to alter the index assignment. In the case of initially slack nanotubes, the substrate was first heated until the Rayleigh peaks began to shift. In all of the devices studied, the strain effects were completely reversible, indicating an absence of slippage at the contact points.

Figure 2 shows Rayleigh spectra for three types of nanotubes under varying axial strains up to $\varepsilon = 2\%$. Figure 2(a) shows data for a (20,12) semiconducting nanotube. The two peaks, corresponding to the third (S_{33}) and fourth (S_{44}) optical transitions, shift monotonically with applied strain, but in opposite directions. For the case of the (19,13) chiral metallic nanotube of Fig. 2(b), we observe a feature arising from the second transition (M_{22}), which is split into upper ($M_{22}{}^{+}$) and lower ($M_{22}{}^{-}$) levels by the trigonal warping effect [19]. The two levels shift toward each other under applied strain. Similar behavior was observed in a second chiral metallic nanotube (21,9). The spectrum for the high-symmetry (16,16) armchair metallic nanotube of Fig. 2(c) displays a single degenerate M_{22} peak. This peak shifts upward slightly with strain, an effect also observed in a second (17,17) armchair nanotube.

In a picture of noninteracting electrons, the optical transitions in nanotubes are vertical transitions between the 1D bands that arise from quantized slices of the 2D graphene band structure. Although more detailed analysis shows that the optical transitions are excitonic in nature [20], the single-electron picture predicts the transition energies reasonably well [21] and will be used in our discussion. The tight-binding model developed by Yang and Han [3] predicts that axial strain shifts the Fermi point of a

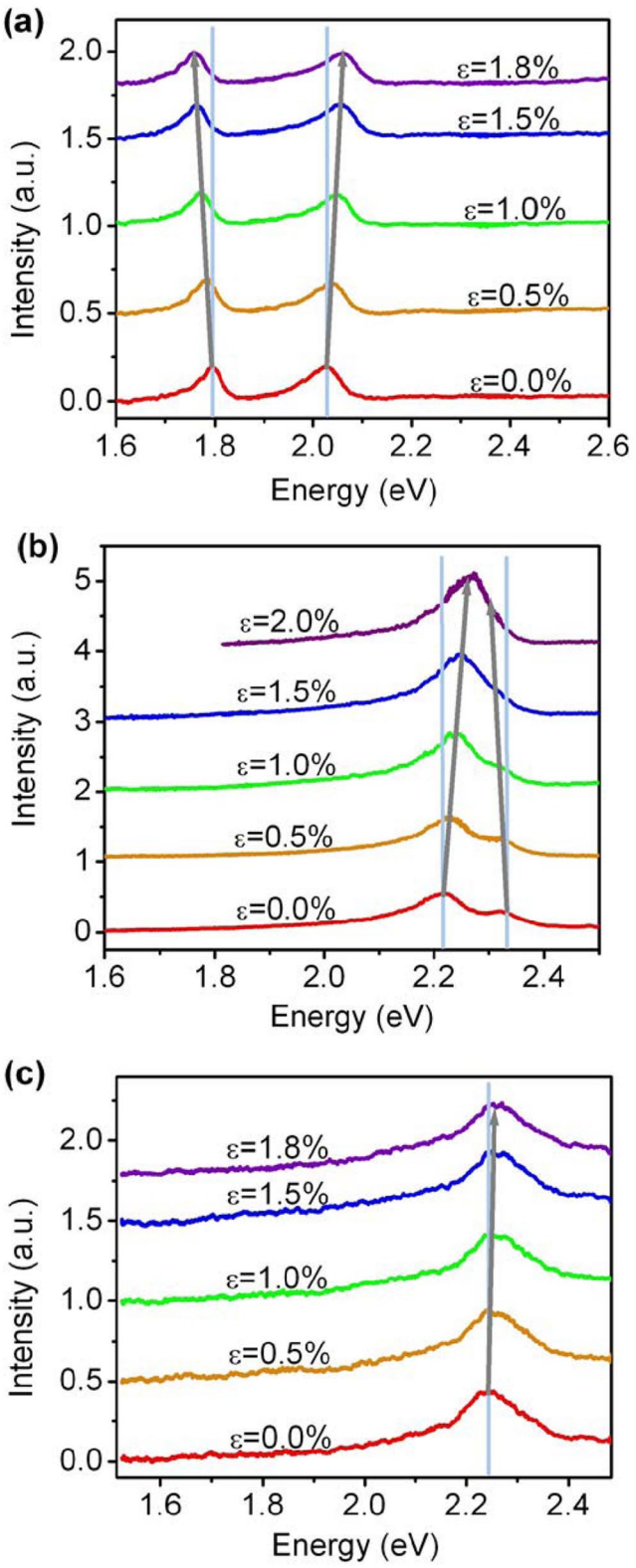

FIG. 2 (color online). Rayleigh scattering spectra for nanotubes under axial strain, displaced vertically by a distance corresponding to the applied strain. The gray line traces the shift in the transition energy. Results are shown for (a) a semiconducting (20,12) nanotube, (b) a (19,13) chiral metallic nanotube, and (c) a (16,16) armchair metallic nanotube.

graphene sheet outward from the K point, with the perpendicular component of the shift given by

$$\Delta k_F^c = \frac{2}{3t_0 a_{c-c}} \sum_{i=1}^{3} \cos\left(\theta + \frac{2i\pi}{3}\right) \cdot \Delta t_i \qquad (1)$$

where θ is the chiral angle. In this expression, t_0 is the graphene tight-binding overlap integral for the nearest-neighbor π-bonds, evaluated at the equilibrium bond length a_{c-c}. Δt_i denotes the change of overlap integral of the ith bond as a result of the applied strain, obtained from the simple model of $t = t_0(a_{c-c}/R)^2$ [22] for the interaction strength as a function of the C-C bond length R. Assuming that the lattice acts as an elastic medium with Poisson ratio ν, one then obtains for the change in the band gap ΔE induced by uniaxial strain ε

$$\frac{\Delta E}{\varepsilon} = \mathrm{sgn}(2p+1)3t_0(1+\nu)\cos(3\theta). \qquad (2)$$

Here, the factor $p = 0$ (metallic) and ± 1 (semiconducting) satisfies $p = n - m - 3q$, where q is an integer and describes the nanotube family.

To compare theory with our measurements, we generalize this expression to include the higher-lying optical transitions. Because of the nearly linear dispersion of graphene near the Fermi point, the strain-induced energy shifts should be essentially identical in magnitude for every transition. Successive higher-order optical transitions, however, originate from lines on alternating sides of the K point. Therefore, the Fermi point displacement will alternately increase and decrease successive transition energies. For the E_{kk} transitions, we thus obtain

$$\frac{\Delta E_{kk}}{\varepsilon} = \mathrm{sgn}(2p+1)(-1)^{k+1}3t_0(1+\nu)\cos(3\theta). \qquad (3)$$

Within this framework, the M_{ii}^{+} and M_{ii}^{-} metallic peaks are associated with $k = 2i$ and $k = 2i - 1$, respectively. The split metallic peaks are expected to approach one another under strain. For the single resonance of armchair metallic nanotubes, the chiral angle is $\theta = \pi/6$, and no strain-induced shift is predicted at this level of analysis.

The behavior observed for the five measured nanotubes shows qualitative agreement with the above theory. For the semiconducting (20,12) nanotube, $p = -1$; Eq. (3) predicts that E_{33} will shift downward and E_{44} upward, consistent with the observed behavior. For the two chiral metal tubes, $p = 0$, and the M_{22}^{-} ($k = 3$) and M_{22}^{+} ($k = 4$) peaks should approach one another, as seen experimentally. Finally, the two armchair nanotubes exhibit only very slight strain-induced shifts. Theory predicts no shift, and the small observed effect must arise from corrections beyond those considered in this analysis.

A more quantitative comparison of experiment and theory is presented in Fig. 3. The solid points show the measured strain-induced shift, $\Delta E/\varepsilon$, for each transition, plotted versus the structural factors on the right side of Eq. (3). The solid line shows theoretical prediction of

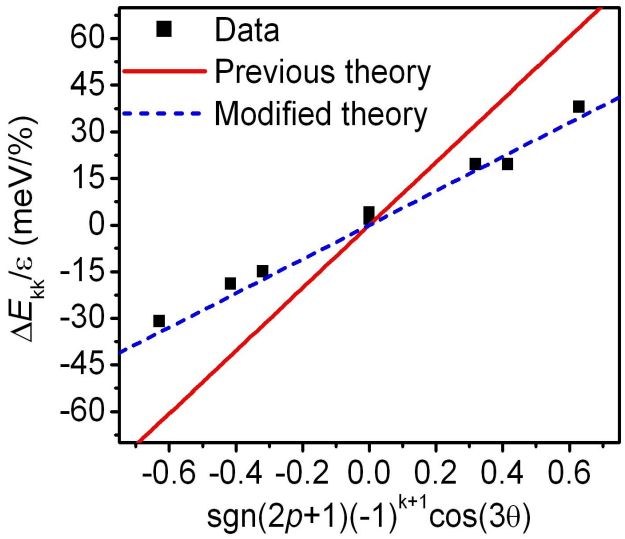

FIG. 3 (color online). Shift rates for the measured nanotube electronic transitions, plotted against the parameter $\mathrm{sgn}(2p+1)(-1)^{k+1}\cos(3\theta)$ that is expected to normalize for the nanotube structure and for the optical transition number k. The solid squares show experimental results for the all accessible transitions in the 5 measured nanotubes. The existing theoretical prediction [Eqn. (3)] is shown as a solid line, with the modified theoretical prediction [Eqn. (6)] as a dashed line.

Eq. (3), using $t_0 = 2.7$ eV, which provides a good fit to the band structure near the Fermi point [23], and $\nu = 0.2$ [9]. The theory correctly predicts that data for different nanotubes and different transitions all collapse into a single line. However, the slope is smaller than predicted by nearly a factor of 2.

The Cauchy-Born rule, used in the previous theoretical treatment, assumes that the positions of *all* of the atoms in a material subject to a homogeneous deformation follow a single mapping from the undeformed to the deformed configuration [24]. However, this rule is not valid for graphitic carbon, whose hexagonal structure comprises two triangular sublattices. As was recently explored by Nisoli *et al.* [25], we must also include an internal relaxation displacement $\boldsymbol{r}$ between the two sublattices (each of which deforms homogeneously and identically). This sublattice relaxation will affect the change Δt_i in the overlap integrals in Eqn. (1) and, hence, the predicted shift in the band gap ΔE.

We determine the relaxation of one sublattice relative to the other by minimizing the elastic energy of the system, using a model of nearest-neighbor atomic interaction potentials consisting of bond-stretching and bond-bending terms. To this end, consider a unit cell with a carbon atom at the origin in which atoms in the complementary sublattice fixed. The strain-induced changes $\Delta\mathbf{R}_i$ of the bond vectors $\mathbf{R}_i$ for the three nearest-neighbor atoms are given by a combination of the overall deformation and the relaxation displacement vector $\boldsymbol{r}$: $\Delta\mathbf{R}_i = F\mathbf{R}_i - \mathbf{r}$, where

F is the displacement gradient tensor. The potential energy of the unit cell is then

$$E_{\text{cell}} = \frac{1}{2}\sum_{i=1}^{3}[k_r|\Delta\mathbf{R}_i|^2 + 2k_\varphi(\Delta\varphi_i)^2]. \quad (4)$$

Here, $i = 1, 2, 3$ extends over the three nearest neighbors and $\Delta\varphi_i$ denotes the strain-induced change in angle of the ith bond. By minimizing E_{cell} with respect to the relaxation vector $\boldsymbol{r}$, we find

$$\vec{r} = \frac{1-6\alpha}{2(1+6\alpha)}(1+\upsilon)\varepsilon a_{c-c}[-\sin(3\theta)\vec{c} + \cos(3\theta)\vec{t}], \quad (5)$$

where $\alpha = k_\phi/k_r a_{c-c}^2$ and $\vec{c}$ and $\vec{t}$ denote, respectively, the circumferential and axial unit vectors for the nanotube. In the analysis below, we choose $\alpha = 0.066$, based on $k_r = 652$ nN/nm and $k_\phi = 0.87$ nN nm [26], values that have been previously applied to predict the measured bulk mechanical properties of nanotubes [27,28].

Having obtained the sublattice relaxation under applied axial strain, we must consider how this affects the electronic structure. We can modify the previous theory [3] simply by calculating the change in the overlap integrals $\Delta t_i = t(\mathbf{F}\vec{R}_i - \vec{r}) - t_0 = \Delta t_i^0 - \Delta t_i(\vec{r})$ for the corrected atomic positions. Equation (5) then yields the strain-induced change in the band gap:

$$\frac{\Delta E_{kk}}{\varepsilon} = \frac{12\alpha}{1+6\alpha}\text{sgn}(2p+1)(-1)^{k+1}(1+\upsilon)3t_0\cos(3\theta). \quad (6)$$

Equation (6) is identical to the original expression of Eqn. (3), except for the prefactor $12\alpha/(1+6\alpha) = 0.57$. Figure 3 shows that the modified theory predicts the experimental results directly without any adjustable parameters.

To summarize, we have successfully investigated the strain-induced change of band structure of individual nanotubes of known chiral index. Previous theoretical predictions were confirmed qualitatively but shown to be inaccurate quantitatively. This disagreement could be eliminated by taking into account the relative relaxation of one sublattice of carbon atoms in the graphene structure with respect to the other. A direct implication of the study is in analysis of the coupling between the electronic system and any long-wavelength acoustic phonon. The associated scattering rate is governed by the square of the deformation potential [29,30], which describes the change in energy induced by the strain field of the phonon. From the present Letter, we see that neglecting inter-sublattice relaxation will cause the predicted deformation potential to be substantially too high and, hence, to predict a scattering rate that is too great.

We acknowledge support from the Nanoscale Science and Engineering Initiative of the NSF under Grant Nos. ECS-05-07111 and CHE-0117752, Intel Corporation, and the DARPA Center on Nanoscale Science and Technology for Integrated Micro/Nano-Electromechanical Transducers (iMINT, Grant No HR0011-06-1-0048).

[1] R. Saito, G. Dresselhaus, and M. S. Dresselhaus, *Physical Properties of Carbon Nanotubes* (Imperial College Press, London, 2001).
[2] L. Yang *et al.*, Phys. Rev. B **60**, 13874 (1999).
[3] L. Yang and J. Han, Phys. Rev. Lett. **85**, 154 (2000).
[4] A. Maiti, A. Svizhenko, and M. P. Anantram, Phys. Rev. Lett. **88**, 126805 (2002).
[5] R. B. Capaz *et al.*, Phys. Status Solidi B **241**, 3352 (2004).
[6] A. G. Souza *et al.*, Phys. Rev. Lett. **95**, 217403 (2005).
[7] E. D. Minot *et al.*, Phys. Rev. Lett. **90**, 156401 (2003).
[8] T. W. Tombler *et al.*, Nature (London) **405**, 769 (2000).
[9] J. Cao, Q. Wang, and H. J. Dai, Phys. Rev. Lett. **90**, 157601 (2003).
[10] R. J. Grow *et al.*, Appl. Phys. Lett. **86**, 093104 (2005).
[11] H. Maki, T. Sato, and K. Ishibashi, Nano Lett. **7**, 890 (2007).
[12] M. Y. Sfeir *et al.*, Science **306**, 1540 (2004).
[13] M. Y. Sfeir *et al.*, Science **312**, 554 (2006).
[14] S. M. Bachilo *et al.*, Science **298**, 2361 (2002).
[15] C. Fantini *et al.*, Phys. Rev. Lett. **93**, 147406 (2004).
[16] L. M. Huang *et al.*, J. Phys. Chem. B **110**, 11103 (2006).
[17] Y. Maniwa *et al.*, Phys. Rev. B **64**, 241402 (2001).
[18] Y. Wu *et al.* (to be published).
[19] R. Saito, G. Dresselhaus, and M. S. Dresselhaus, Phys. Rev. B **61**, 2981 (2000).
[20] F. Wang *et al.*, Science **308**, 838 (2005).
[21] G. Dukovic *et al.*, Nano Lett. **5**, 2314 (2005).
[22] W. A. Harrison, *Electronic Structure and the Properties of Solids: the Physics of the Chemical Bond* (Dover Publications, New York, 1989), p. xx.
[23] S. Reich *et al.*, Phys. Rev. B **66**, 035412 (2002).
[24] M. Born and K. Huang, *Dynamical Theory of Crystal Lattices* (Clarendon Press, Oxford, 1954), p. xii.
[25] C. Nisoli *et al.*, Phys. Rev. Lett. **99**, 045501 (2007).
[26] W. D. Cornell *et al.*, J. Am. Chem. Soc. **117**, 5179 (1995).
[27] C. Y. Li and T. W. Chou, Int. J. Solids Struct. **40**, 2487 (2003).
[28] G. M. Odegard *et al.*, Compos. Sci. Technol. **62**, 1869 (2002).
[29] J. Y. Park *et al.*, Nano Lett. **4**, 517 (2004).
[30] H. Suzuura and T. Ando, Phys. Rev. B **65**, 235412 (2002).